Quantitative ^{31}P HR-MAS MR spectroscopy for detection of response to PI3K/mTOR inhibition in breast cancer xenografts

Running title: Quantitative ^{31}P HR-MAS MRS

Author list:

Morteza Esmaeili[1*]

Tone F. Bathen[1,2]

Olav Engebråten[3,4]

Gunhild M. Mælandsmo[3]

Ingrid S. Gribbestad[1]

Siver A. Moestue[1,2]

[1] Department of Circulation and Medical Imaging, Norwegian University of Science and Technology (NTNU), P.O. Box 8905, N-7491 Trondheim, Norway.

[2] St. Olavs University Hospital, P.O. Box 3250 Sluppen, N-7006, Trondheim, Norway.

[3] Department of Tumor Biology, Institute for Cancer Research, Oslo University Hospital HF-Radiumhospitalet, Montebello, N-0310 Oslo, Norway.

[4]Department of Oncology, Oslo University Hospital HF – Ullevaal, and Institute for Clinical Medicine, University of Oslo (UiO), P.O. Box 1171 Blindern, N-0318 Oslo, Norway.

*Corresponding author:

Morteza Esmaeili

Email: m.esmaeili@ntnu.no

Address: NTNU/ISB, P.O.Box 8905, 7491, Trondheim, Norway

Keywords: (Max 6 words)

choline metabolism, phospholipid, absolute quantification, phospholipase A2, ethanolamine, glycerophosphocholine

ABSTRACT

PURPOSE:

Phospholipid metabolites are of importance in cancer studies, and have been suggested as candidate metabolic biomarkers for response to targeted anticancer drugs. The purpose of this study was to develop a phosphorus (^{31}P) high resolution magic angle spinning (HR-MAS) magnetic resonance spectroscopy (MRS) protocol for quantification of phosphorylated metabolites in intact cancer tissue.

METHODS:

^{31}P spectra were acquired on a 14.1 T spectrometer with a triplet ^{1}H/^{13}C/^{31}P MAS probe. Quantification of metabolites was performed using the PULCON principle. Basal-like and luminal-like breast cancer xenografts were treated with the dual PI3K/mTOR inhibitor BEZ235, and the impact of treatment on the concentration of phosphocholine (PCho), glycerophosphocholine (GPC), phosphoethanolamine (PEtn) and glycerophosphoethanolamine (GPE) was evaluated.

RESULTS:

In basal-like xenografts, BEZ235 treatment induced a significant decrease in PEtn (-25.6%, $P = 0.01$) whilst PCho (16.5%, $P = 0.02$) and GPC (37.3%, $P < 0.001$) were significantly increased. The metabolic changes could partially be explained by increased levels of phospholipase A2 group 4A (PLA2G4A).

CONCLUSION:

^{31}P HR-MAS MRS is a useful method for quantitative assessment of metabolic responses to PI3K inhibition. Using the PULCON principle for quantification, the levels of PCho, GPC, PEtn and GPE could be evaluated with high precision and accuracy.

INTRODUCTION

High resolution magic angle spinning (HR-MAS) magnetic resonance spectroscopy (MRS) possesses a great diagnostic potential in cancer, as the levels of diagnostically important metabolites can be examined in intact tissue samples (1). The metabolic profiles of the tissue directly reflect the in vivo status of cancer metabolism and its relationship with the underlying tumor biology. ^{1}H MRS is the most sensitive MRS methodology and is frequently used for investigating the metabolic profiles and changes associated with cancer (1-4). Quantitative ^{31}P HR-MAS MRS is rarely used, and has never been used to quantify the levels of phosphorylated metabolites in breast cancer tissue. One of the main reasons is the lower intrinsic sensitivity of ^{31}P MRS. Compared with ^{1}H HR-MAS MRS, larger tissue specimens are needed and the total analysis time is longer. In this study we developed a quantitative ^{31}P HR-MAS MRS protocol which can be used for ex vivo analysis of breast cancer tissue taking these limitations into account.

Choline-containing metabolites (choline, phosphocholine (PCho), and glycerophosphocholine (GPC)) are of special interest in breast cancer (5) due to the abnormal choline metabolism. The choline metabolites have been suggested as diagnostic biomarkers, but may also play a role in therapy monitoring (6). The role of ethanolamine-containing metabolites is still not fully understood. Phosphoethanolamine (PEtn) and glycerophosphoethanolamine (GPE) have potential clinical relevance and have been suggested as biomarkers for diagnosis and response to targeted anticancer drugs (7-10). Choline- and ethanolamine-containing metabolites resonances overlap in one dimensional (1D) ^{1}H HR-MAS MR spectra and the weak resonances from PEtn and GPE are difficult to detect. However, ^{31}P MRS is associated with less background signal and provides a wider chemical shift dispersion enabling spectral separation of both choline- and ethanolamine-containing metabolites. ^{31}P

MRS may therefore allow detailed studies of phospholipid metabolism in breast cancer, with a potential for translation to in vivo applications.

Breast cancer can be divided into subtypes with different clinical characteristics, based on the gene expression profile (11). Basal-like breast cancer has a poor prognosis, and is frequently associated with lacking expression of the steroid hormone receptors; estrogen receptor (ER) and progesterone receptor (PgR) and the human epidermal growth factor receptor 2 (HER2) (11,12). Treatment of this type of breast cancer is challenging due to lack of molecularly targeted drugs (13). Relevant preclinical models are therefore required for development and evaluation of novel anti-cancer drugs, and for identification of treatment response biomarkers (6,14).

The phosphatidylinositol-3-kinase/mammalian target of the rapamycin (PI3K/mTOR) signaling pathway promotes cell proliferation and survival, but it is also directly involved in regulation of cellular metabolism (15). Drugs targeting the PI3K signaling pathway have shown potential in anticancer treatment and may be of particular benefit in basal-like breast cancer (16,17). Several candidate drugs are currently in clinical trials (17). Noninvasive, in vivo assessment of metabolic response to treatment with this novel class of drugs can improve their clinical utility through rapid identification of responding patients, and in vitro studies have identified several potential metabolic biomarkers for response to PI3K inhibition (18-20). In this study, we used ^{31}P HR-MAS MRS to identify phosphorylated biomarkers for response to treatment with the dual PI3K/mTOR inhibitor BEZ235 in tissue samples obtained from two patient-derived breast cancer xenograft models representing basal-like and luminal-like breast cancer.

METHODS

Animals

The xenograft models from two genetically distinct human breast cancer subtypes representing basal-like (MAS98.12) and luminal-like (MAS98.06) breast cancer were established by direct implantation of primary human breast cancer tissues in the mammary fat pad of immunodeficient mice, and then serially transplanted in BalbC nu/nu mice (21). The animals used in this study were housed under pathogen free environment in individually ventilated cages. Housing conditions included an equal light/dark cycle and room temperature of 19 – 22 ˚C. The drinking water was supplemented with 17-β-estradiol (4 μg/ml) to promote growth of the ER-positive luminal-like xenografts. The mice (10 basal- and 6 luminal-like xenografts) received 50 mg/kg of the dual PI3K/mTOR inhibitor BEZ235 (Selleck Chemicals, Houston, TX, USA) dissolved in vehicle (30% Captisol/NMP 66:33 v/v) by gavage daily for three days. Control animals (11 animals; 6 basal- and 5 luminal-like xenografts) received volume-matched drug free vehicle only. These dose levels have previously shown efficacy in murine xenograft models (22). In a previous study, it has been shown that the basal-like xenograft model responds to treatment with BEZ235 whereas no response was seen in the luminal-like xenograft model (23). After treatment, the animals were sacrificed by cervical dislocation and tumors were harvested and immediately snap-frozen in liquid nitrogen. Harvested tumor tissues were stored in liquid nitrogen until HR-MAS MRS analysis.

All procedures and experiments involving animals were approved by The National Animal Research Authority, and carried out according to the European Convention for the Protection of Vertebrates used for Scientific Purposes.

Preparation of tumor specimens for HR-MAS analysis

HR-MAS MRS was carried out on a spectrometer (Bruker Avance III 600 MHz/54 mm US-Plus) equipped with a Triplet $^{1}H/^{13}C/^{31}P$ MAS probe (Bruker BioSpin GmbH, Ettlingen, Germany). Frozen tumor specimens (24.2 ± 4.6 mg) were thawed, cut on an ice-pad, and gently loaded into 30 µl disposable inserts filled with 3 µl deuterium oxide (D_2O, Sigma-Aldrich GmbH, Germany) to ensure the ^{2}H lock. The inserts were then placed into 4mm diameter ZrO_2 MAS rotors (Bruker BioSpin GmbH, Ettlingen, Germany). The MAS rotors were spun at 5 kHz and maintained at 4˚C to minimize enzymatic activities within the tissue samples. The actual temperature of the probe was calibrated periodically using a 4% methanol-d4 standard (Bruker GmbH, Germany). Shimming and carrier frequency adjustments were performed 5 minutes after transfer of the sample to the magnet to ensure temperature equilibrium.

^{31}P HR-MAS MRS

^{31}P HR-MAS spectra were acquired using an inverse-gated ^{31}P pulse-acquired sequence with ^{1}H decoupling activated during the acquisition (Bruker; zgig), eliminating ^{1}H-^{31}P coupling without nuclear overhauser effect (NOE) build-up. Acquisition parameters consisted of a 30˚ excitation pulse, 1536 transients, 32 K complex data points, 60 ppm spectral width, acquisition time of 1.12 s, recovery delay of 2.5 s (a repetition time of 3.62 s), and a total acquisition time of 1 hr 30 min.

Longitudinal ^{31}P Relaxation time (T1)

Longitudinal ^{31}P relaxation studies were performed in five tumor specimens using an inversion recovery pulse sequence (Bruker; t1ir). For each measurement, 6K complex data points were collected over a spectral width of 12 ppm, with an acquisition time of 1.05 s, recovery delay of 10 s, and 4 transients per delay time. The inversion recovery experiment lasted 1 hr 5 min, consisting of 4 delay times ranging from 50 ms to 10 s. The relaxation times

were used to determine the optimal repetition time for quantitative ^{31}P MRS acquisition, minimizing the total acquisition time but avoiding resonance saturation.

Degradation Analysis

^{1}H HR-MAS spectra were acquired before and after each ^{31}P MR acquisition to investigate the possible metabolic degradation. The spectra were acquired using a Carr-Purcell-Meiboom-Gill (CPMG) pulse sequence (Bruker; cpmgpr1d) including a MAS rotor synchronized T2 filter (to attenuate macromolecule and lipid resonances and suppress water resonances) followed by a 90˚ excitation pulse, over a spectral width of 20 ppm, and 136 ms spin echo time. A total of 64 transients were collected into 64K complex data points, acquisition time of 2.73 s, recovery delay of 10 s (a repetition time of 12.73 s), and a total acquisition time of 7 min. Data preprocessing was performed in Matlab 7.10.0.499 (The Mathworks, Inc., Natick, MA, USA), and the changes in areas of PCho and GPC signals were calculated in the two ^{1}H MR spectra.

Data Processing

The ^{31}P HR-MAS spectra were processed using TopSpin V 3.0 (Bruker BioSpin GmbH, Ettlingen, Germany). The raw data were multiplied by a 3 Hz exponential weighting function prior to Fourier transformation. All spectra were processed using automatic phase and baseline correction routines. The chemical shifts in the HR-MAS spectra were calibrated to the GPC peak at 3.04 ppm for ^{31}P and the lactate doublet at 1.34 ppm for ^{1}H. GPC has previously been shown to have a stable chemical shift in ^{31}P HR-MAS experiments (24). The area under the metabolite and methylenediphosphonic acid (MDPA, Sigma-Aldrich GmbH, Germany) resonances was calculated using PeakFit software (PeakFit V 4.12, SeaSolve Software Inc., San Jose, CA, USA). A Voigt curve fitting function (25), which is a mixed Gaussian-Lorenzian lineshape model, was used after baseline refinement. The fit correlation factor (r^2) was better

than 0.99 for all spectra. Relaxation time raw data were processed using the T1 calculation of the TopSpin V 3.0 software.

Quantification

Phosphorylated metabolites were quantified using the PULCON principle (26). MDPA was used as an external reference. To investigate the precision and accuracy of quantification using the PULCON principle, disposable inserts were filled with three different MDPA reference standard solutions (7.09, 29.01, and 49.64 µmol/g). Five replicates of each concentration were analyzed to evaluate the analytical precision. To determine the linearity and accuracy of the method, the MDPA concentration was calculated from the MR spectra using equation [1]:

$$[MDPA_{measured\ conc.}] = \frac{A_{MDPA}}{A_{MDPAref}} \times [MDPA_{ref}] \quad (1)$$

A_{MDPA} represents the fitted areas of the MDPA signal in the solutions of various concentrations. $A_{MDPAref}$ represents the fitted area of the $MDPA_{ref}$ signal in the reference standard sample, defined as the MDPA reference standard solution with the lowest concentration ($[MDPA_{ref}]$ = 7.09 µmol/g).

The accuracy of the external reference was calculated using equation [2], and the precision was described by the standard deviation calculated for each of the 3 different concentrations of the MDPA solutions.

$$Relative\ error = 100 \times \frac{|MDPA_{actual\ conc.} - MDPA_{measured\ conc.}|}{MDPA_{actual\ conc.}} \quad (2)$$

The concentration of the choline- and ethanolamine-containing metabolites in the tissue samples ([*Met*]) were calculated using equation [3]:

$$[Met] = \frac{A_{Met}}{A_{MDPA}} \times \frac{n_{MDPA}}{n_{Met}} \times \frac{MDPA}{weight_{tissue}} \quad (3)$$

A_{Met} and A_{MDPA} are the fitted areas of the metabolite of interest and the MDPA signal, respectively. n_{Met} and n_{MDPA} represent the number of phosphorus nuclei giving rise to the MR signals from the metabolite of interest and MDPA signal, respectively. *MDPA* is the mean amount of MDPA in the reference standard with lowest concentration (= 0.23 µmol), and $weight_{tissue}$ is the analyzed tissue mass.

Western Blot Analysis

To explain changes in PCho, PEtn, and GPC, enzymes directly involved in synthesis of these metabolites were investigated. Antibodies for PLA2G4A (SC-454), choline kinase A (ChoKA, SC-376489), choline kinase B (ChoKB, SC-86382), ethanolamine kinase 1 (ETNK1, SC-130754), and ethanolamine kinase 2 (ETNK2, SC-162780) purchased from Santa Cruz Biotechnology (Santa Cruz, CA, USA) were used to measure the expression of these proteins. In addition, β-actin (ab8226, AbCam, Cambridge, UK) was used as a loading control.

After HR-MAS MRS analysis, proteins were extracted from BEZ235-treated and vehicle control basal-like xenograft tissue using a pestle homogenizer in RIPA (radio immuno precipitation assays) buffer (SC-24948, Santa Cruz Biotechnology, Santa Cruz, CA, USA) with 2 mM PMSF (phenylmethanesulfonyl fluoride), 1 mM Na-orthovanadat and 10 µl/ml Protease inhibitormix (Santa Cruz Biotechnology, Santa Cruz, CA, USA). After 20 min extraction at 4ºC the protein lysate was clarified at 10000 g for 10 min.

50 µg protein extract was separated using 1D PAGE (P antigen family) with 4-12% NuPage Novex Bis-Tris gels using MOPS run buffer (Invitrogen, Carlsbad, USA). The gels were electro-blotted on nitrocellulose. The membranes were blocked for 3 hr in TBS, 0.1% Tween (TBST), 5% fat-free dry milk and incubated in primary antibody for 1 hr in blocking

buffer. After 3 x 10 min washing in TBST, membranes were further incubated for 1 hr in secondary fluorescent-conjugated (LI-COR Biosciences, NE, USA) antibodies in TBST, washed 3 x 10 min TBST and 1 x 10 min TBS. The gels were scanned on an Odyssey imaging system (LI-COR Biosciences, NE, USA) and bands were quantified by densitometry using ImageStudio 2.0 software.

Statistical Analysis

Statistical analyses were performed using GraphPad Prism (GraphPad Software, Inc. V 4.03, CA, USA). Spearman correlation analysis was performed between actual and measured MDPA concentrations. Metabolite concentrations were compared across treatment groups using the non-parametric Mann-Whitney test with the threshold for statistical significance defined as $P \leq 0.05$.

RESULTS

^{31}P HR-MAS MR spectra with high spectral resolution and good signal to noise ratio were obtained from all tissue samples. Resolved resonances from PEtn, PCho, inorganic phosphate (Pi), GPE, and GPC were identified between 3.04 – 6.70 ppm (Figure 1). A distinct signal (at 6.76 ± 0.05 ppm) was observed in the ^{31}P MR spectra of treated tissue samples. Based on previous knowledge (27,28), this signal was assigned to glycerol 3-phosphate (G3P). There was no significant contribution from high energy phosphate metabolites such as phosphocreatine and adenosine triphosphates in the ^{31}P MR spectra, reflecting the rapid metabolism and degradation of these metabolites.

Longitudinal Relaxation Times and MDPA Calibration

The longitudinal relaxation times (T1) of the phosphorylated metabolites were determined using an inversion recovery pulse sequence. The resulting T1 values (presented in Table 1) confirm that a repetition time of 3.62 s (> 5 × T1) is sufficient for quantitative analysis of the phosphorous metabolites. A significant correlation (P < 0.0001 and r = 0.96) was observed between actual and measured MDPA concentrations (Figure 2A), demonstrating a linear concentration-response relationship. The accuracy of quantification using the PULCON principle was calculated using the lowest MDPA concentration (= 7.09 µmol/g) as reference. The relative error was < 4.31 % at all concentrations (Figure 2B), demonstrating a high level of precision in a concentration range representative of phosphorylated metabolites in xenograft tumor tissues.

Metabolite stability

^{1}H HR-MAS spectra of tissue samples from both BEZ235 treated and control groups indicated an increase in PCho and GPC concentration during the acquisition of ^{31}P spectra at 4 ºC. The changes in PCho and GPC concentrations are presented in Table 2. The PCho level increased significantly more in basal-like than in luminal-like xenografts. However, there was no significant difference in metabolite stability between controls and treated mice in any of the xenograft models, justifying that metabolite concentrations can be compared across the treatment groups.

^{31}P MR Spectral Profiles in Breast Cancer Xenografts

^{31}P HR-MAS spectra were analyzed to investigate the effect of PI3K/mTOR pathway inhibition on choline- and ethanolamine-containing metabolites. Representative spectra from luminal-like and basal-like xenografts are presented in Figure 1, showing well resolved peaks from phosphorylated metabolites and metabolic changes associated with BEZ235 treatment. The ^{31}P MR spectra showed distinct differences between luminal-like and basal-like xenograft

models, confirming an inverse relationship in PCho-GPC concentrations which is also seen in previous studies (29). The concentrations of phosphorylated metabolites in basal-like and luminal-like xenografts are presented in Figure 3. In samples from basal-like xenografts treated with BEZ235, a significant reduction in PEtn concentration (-25.6%, $P = 0.01$) compared to vehicle treated controls was observed (Figure 3). Treatment with BEZ235 also induced a significant increase in PCho (16.5%, $P = 0.02$) and GPC (37.3%, $P < 0.001$) (Figure 1 and 3). In the luminal-like xenografts, BEZ235 treatment induced no significant change in the concentration of phosphorylated metabolites.

PI3K/mTOR Pathway Inhibition Effects on Enzymatic Activities

Western blot analysis was performed to further investigate the effect of PI3K/ mTOR pathway inhibition on phospholipid metabolism in basal-like xenografts. No difference in protein expression of ChoKA, ChoKB, ETNK1, or ETNK2 between BEZ235-treated mice and vehicle-treated controls was observed. However, a 2-fold increase in the PLA2G4A levels ($P = 0.005$) in treated tissue samples compared to vehicle-treated controls was observed (Figure 4). PLA2G4A has previously been associated with the high GPC concentration observed in the basal-like xenograft model (29).

DISCUSSION

In this study, we have established a quantitative ^{31}P HR-MAS MRS protocol for assessment of phosphorylated metabolites in breast cancer xenograft tissue. We have demonstrated the feasibility of the method in metabolic profiling of breast cancer subtypes, and for assessment of metabolic response to a dual PI3K/mTOR inhibitor. Treatment of the basal-like breast cancer xenograft model was associated with increased concentrations of PCho and GPC and decreased concentration of PEtn. After HR-MAS analysis, the intact tissue samples

were used for Western blot analyses, which suggested that the metabolic changes in part could be attributed to a change in PLA2G4A levels.

Quantitative performance of the ^{31}P HR-MAS MRS protocol

The implemented ^{31}P HR-MAS MRS protocol uses the PULCON principle for quantification (30). The concentration of metabolites present in the sample is determined using the reference spectrum of an external standard with known concentration obtained under identical experimental conditions. Advances in spectrometer technology have enhanced the stability and reproducibility, thereby allowing direct quantitative analysis. The linearity of the method was demonstrated by a relative error ≤ 4.31% in the MDPA reference standard solutions. A relative standard deviation < 0.1 % demonstrate a high precision of the measurement. The concentration-response relationship was linear in the range of 7.09 – 49.64 µmol/g. Thus, we consider the performance of the method to be adequate for evaluation of phosphorylated metabolites in tumor tissue samples. Traditionally, quantitative HR-MAS MRS has been performed through addition of internal standards to the sample. This method has several disadvantages such as reduced reproducibility and accuracy due to interaction between the standard and tissue components, as well as pH dependency. The ERETIC (Electronic Reference To access In vivo Concentrations) approach is an alternative to the classical internal standard method, and is based on the use of a synthetic radio frequency reference signal (31). This approach eliminates the need for an internal standard, thereby improving precision and accuracy (32). The absence of the artificial signal generation in the current protocol reduces the number of potential error sources compared to the ERETIC approach. MDPA is a suitable external reference, since its resonance frequency does not overlap with other peaks in the ^{31}P spectra. In summary, the analytical performance of the PULCON-based ^{31}P HR-MAS MRS method is equivalent to that of ERETIC-based protocols (2,32), allowing direct quantification of metabolite concentration in intact tissue.

Metabolite stability

A major source of error in quantitative HR-MAS MRS experiments is metabolite degradation. Metabolite degradation may occur during tissue excision, sample preparation, or during the acquisition of MR spectra. However, immediate freezing, rapid sample preparation and low temperature during HR-MAS MRS analysis can minimize metabolite degradation. Previous studies have shown that the duration of cryogenic storage do not cause significant alteration in metabolic contents (33,34). As the ^{31}P HR-MAS MRS protocol established in this study has a total running time of 1 hr 30 min, degradation of metabolites during the experiment may be a confounding factor. Some metabolic degradation is virtually unavoidable due to high metabolic rates, such as nucleotide triphosphate degradation. We therefore acquired ^{1}H HR-MAS MRS spectra before and after ^{31}P HR-MAS MRS to assess the change in PCho and GPC concentration during analysis. The data clearly indicate that the concentration of PCho and GPC increase over the time course of the ^{31}P HR-MAS MRS acquisition, potentially leading to overestimation of the actual concentration of these metabolites. Metabolite stability therefore has to be taken into account when quantifying phospholipid metabolites. However, our data also demonstrated that the increased levels of PCho and GPC occurred at similar rates in all control and treatment groups (Table 2). The increase was in the range of 10-20 %, which was considered acceptable for evaluation of phospholipid metabolism in xenograft tumors. Although the concentration of metabolites may be overestimated due to increasing levels of PCho and GPC, comparison of metabolite concentrations across treatment groups can be justified.

^{31}P HR-MAS MRS for Evaluation of Cancer Phospholipid Metabolism

A major trend in current cancer drug development is to target specific oncogenic signaling pathways using low molecular weight drugs (35). This class of drugs typically interferes with

proteins involved in signal transduction, resulting in inhibition of tumor growth. In addition, these drugs frequently cause metabolic alterations in the cancer cells (6). However, metabolic responses to therapy may be both drug- and cancer subtype-specific, and there is a need to understand the effects of different drugs on a more detailed level. Therefore, development of methods for evaluation of metabolic responses in preclinical models ex vivo is an important step towards personalized therapy monitoring in patients. The use of MRS to identify metabolic biomarkers can potentially be useful for noninvasive detection of response and resistance, both during preclinical development of novel drugs and in the clinical trial stage. Choline metabolites are widely studied in cancer research as diagnostic biomarkers and indicators of therapeutic response. ^{31}P MRS probes typical membrane phospholipid compounds; PEtn, PCho, GPC, and GPE. These metabolites are suggested as valuable biomarkers in cancer, both for diagnosis/grading and for therapy monitoring (1,5). ^{31}P HR-MAS MRS has previously been employed to investigate intact rhabdomyosarcoma tissues (24) and cervical cancer (36). The amount of tissue required for sufficient signal-to-noise ratio may limit the utility of ^{31}P HR-MAS MRS. In the current study we obtained data from breast tissue samples in the weight range of 24.2 ± 4.6 mg, which is significantly lower than previously reported (24,36).

In this study, we used ^{31}P HR-MAS MRS to demonstrate the metabolic response to PI3K/mTOR inhibition in a basal-like xenograft model. The method could also discriminate between basal-like and luminal-like xenograft models based on ^{31}P-metabolic profiles. The basal-like xenograft model (MAS98.12) responds to BEZ235 treatment, whereas the luminal-like model (MAS98.06) does not (23). Using ^{1}H HR-MAS MRS, Moestue et al. (23) demonstrated that response to PI3K inhibition was associated with decreased glycolytic activity and increased PCho and GPC levels. The increased PCho and GPC levels were confirmed in the present study, but in addition ^{31}P HR-MAS MRS could detect a decrease in PEtn concentrations. The PCho and GPC concentrations found in the two studies are in good

accordance, but the intersubject variability was markedly lower in the ^{31}P HR-MAS MRS data. Since quantification of PCho and GPC in ^{1}H HR-MAS MRS spectra depend on curve fitting of overlapping metabolite peaks, both accuracy and precision may benefit from the use of ^{31}P HR-MAS MRS.

The ^{31}P HR-MAS spectra from basal-like xenografts treated with BEZ235 exhibited an extra peak, which was assigned to G3P based on previous literature (27,28). The underlying biology of the G3P accumulation induced by BEZ235 treatment is not clear. G3P is formed by degradation of GPC, and can feed into the glycolysis after conversion to glyceraldehyde-3-phosphate. Accumulation of G3P could therefore reflect the increased turnover of phosphatidylcholine (as suggested by the increased GPC concentration) and reduced glycolytic activity caused by PI3K/mTOR inhibition. The increased level of PLA2G4A in BEZ235-treated basal-like tumors supports this hypothesis (Figure 4). This phospholipase is commonly found in mammalian tissues and associated with hydrolysis of the sn-2 acyl bond of phosphoglycerides, converting PtdCho to 1-acyl GPC, a precursor of GPC (27). Phospholipases has been shown to be mediators of response to cancer therapy both in vitro and in vivo (37-39). The PLA2GIV gene has previously been shown to be higher expressed in the basal-like xenografts than luminal-like xenografts, and was therefore suggested to be associated with GPC concentration in tumor tissue (29). The increase in PLA2GIV is consistent with the increase in GPC concentration in basal-like tumors treated with BEZ235. This finding is in accordance with previous studies where elevated PLA2 activity was associated with increased GPC concentration in response to the heat shock protein 90-inhibitor 17-AAG (40). Increased PLA2 activity has also been shown to accompany apoptotic cell death (41). PI3K inhibitors may also interfere with the function of enzymes involved in the GPC hydrolysis such as EDI3, an enzyme responsible for cleavage of GPC to produce G3P (27). Small amounts of G3P were also found in samples from luminal-like xenografts treated with BEZ235. Since this xenograft model show

no or little response to treatment with BEZ235, the accumulation of G3P in these tumors is difficult to explain.

We evaluated the impact of the PI3K signaling inhibition on the expression of ChoKA/B and ETNK1/2. No treatment-related changes were observed. The reduction in PEtn observed in BEZ235-treated basal-like tumors is consistent with previously described responses to treatment (10). In contrast, the increased PCho found in the BEZ235-treated basal-like tumors cannot be explained by decreased cell membrane turnover. However, increased PCho has been associated with response to treatment with other targeted drugs such as histone deacetylase inhibitors, illustrating the complexity of choline metabolism in cancer (6). In previous in vitro studies, it has been shown that treatment with PI3K inhibitors cause decreased PCho and increased GPC concentrations (18-20). This is only partly in accordance with the increased PCho and GPC concentrations found ex vivo in our study, which possibly could reflect microenvironmental regulation in metabolite concentrations. However, it has also been shown that PI3K inhibitors can induce apoptosis in breast cancer cells (42). Early event of the apoptosis cascade has been associated with increased levels of PCho and GPC (43). It is therefore possible that the metabolic changes observed in our study reflect BEZ235-induced apoptosis. Metabolic responses to treatment can be mediated by phospholipases C and D, but also other enzymes in the choline metabolism (5,7). In particular, a PtdCho-specific PLC has been suggested to be involved in regulation of PCho concentration in cancer (44). However, the enzyme has not yet been cloned, and specific monoclonal antibodies are not commercially available. We were therefore not able to evaluate the importance of PtdCho-specific PLC in the metabolic response to PI3K inhibition.

Potential of ^{31}P MRS in clinical applications

Clinical in vivo ^{1}H MRS has been used to discriminate between benign and malignant breast lesions, and to monitor response to neoadjuvant therapy by evaluation of the total choline signal (45,46). This method is limited by the lack of spectral resolution, which can obscure changes in individual choline metabolites. Establishing a quantitative ^{31}P HR-MAS MRS to analyze choline metabolism is therefore of particular interest, as it potentially can provide evaluation of individual choline- and ethanolamine-containing metabolites in vivo. These metabolites have potential clinical relevance, but their role as cancer biomarkers are not known in detail. Elevated PEtn concentration is found in most tumor cells (7). The role of GPE is less clear, but in prostate cancer, PEtn and GPE, in contrast to PCho and GPC, can be used to discriminate between cancer and benign prostatic hyperplasia (8,9). PEtn and GPE are also suggested as biomarkers for response to targeted anticancer drugs. In colon cancer xenografts, treatment with the HIF-1 inhibitor PX-478 caused significant reduction in both PEtn and GPE concentration (10).

^{31}P HR-MAS MRS provides more robust quantitative analysis compared to ^{1}H HR-MAS MRS due to the high spectral resolution and the low background signal. However, it has an intrinsically low sensitivity compared to ^{1}H MRS, resulting in longer examination times. The clinical utility of ^{31}P MRS therefore depends on high magnetic field strengths which enhance sensitivity and reduce total scan time. The findings in this study suggest that ^{31}P MRS may be a powerful tool in clinical therapy monitoring of targeted anticancer drugs, by simultaneous assessment of choline- and ethanolamine-containing metabolites. Advances in MR technology and increased availability of clinical high field systems might enable the translation of current ex vivo ^{31}P MRS protocols into in vivo ^{31}P MRS applications.

CONCLUSION

In this study the absolute concentration of phosphorylated metabolites of importance in cancer was calculated using ^{31}P HR-MAS MRS at 14.1T. Based on the PULCON principle, MDPA was used as an external reference, providing higher precision and accuracy compared to other quantitative HR-MAS methods. Using a basal-like and a luminal-like xenograft model, we evaluated the metabolic response to treatment with the dual PI3K/mTOR inhibitor BEZ235. In basal-like xenografts, a significant increase in GPC and PCho was found, whereas PEtn decreased. The increase in GPC could be explained by increased PLA2GIV levels. No significant changes in phosphorylated metabolites were observed in luminal-like xenografts, which do not respond to treatment with BEZ235. This demonstrates that ^{31}P HR-MAS MRS can be a valuable method for detailed studies of phospholipid metabolism in breast cancer.

ACKNOWLEDGEMENTS

The authors thank Alexandr Kristian for his help with animal surgery and Dr. Lars Hagen for his assistance with the western blot analyses. This work was performed at the MR Core Facility, Norwegian University of Science and Technology (NTNU). This project was funded by the Norwegian Cancer Society and the Norwegian Breast Cancer Society (grant number 2209215-2011), the Liaison Committee between the Central Norway Regional Health Authority (RHA, grant number 46056655) and the Norwegian University of Science and Technology (NTNU).

REFERENCES

1. Bathen TF, Sitter B, Sjobakk TE, Tessem MB, Gribbestad IS. Magnetic resonance metabolomics of intact tissue: a biotechnological tool in cancer diagnostics and treatment evaluation. Cancer Res 2010;70(17):6692-6696.
2. Sitter B, Bathen TF, Singstad TE, Fjosne HE, Lundgren S, Halgunset J, Gribbestad IS. Quantification of metabolites in breast cancer patients with different clinical prognosis using HR MAS MR spectroscopy. NMR Biomed 2010;23(4):424-431.
3. Cao MD, Sitter B, Bathen TF, Bofin A, Lonning PE, Lundgren S, Gribbestad IS. Predicting long-term survival and treatment response in breast cancer patients receiving neoadjuvant chemotherapy by MR metabolic profiling. NMR Biomed 2012;25(2):369-378.
4. Cao MD, Giskeodegard GF, Bathen TF, Sitter B, Bofin A, Lonning PE, Lundgren S, Gribbestad IS. Prognostic value of metabolic response in breast cancer patients receiving neoadjuvant chemotherapy. BMC Cancer 2012;12:39.
5. Glunde K, Bhujwalla ZM, Ronen SM. Choline metabolism in malignant transformation. Nat Rev Cancer 2011;11(12):835-848.
6. Moestue SA, Engebraaten O, Gribbestad IS. Metabolic effects of signal transduction inhibition in cancer assessed by magnetic resonance spectroscopy. Mol Oncol 2011;5(3):224-241.
7. Podo F. Tumour phospholipid metabolism. NMR Biomed 1999;12(7):413-439.
8. Swanson MG, Keshari KR, Tabatabai ZL, Simko JP, Shinohara K, Carroll PR, Zektzer AS, Kurhanewicz J. Quantification of choline- and ethanolamine-containing metabolites in human prostate tissues using 1H HR-MAS total correlation spectroscopy. Magn Reson Med 2008;60(1):33-40.
9. Komoroski RA, Holder JC, Pappas AA, Finkbeiner AE. 31P NMR of phospholipid metabolites in prostate cancer and benign prostatic hyperplasia. Magn Reson Med 2011;65(4):911-913.
10. Jordan BF, Black K, Robey IF, Runquist M, Powis G, Gillies RJ. Metabolite changes in HT-29 xenograft tumors following HIF-1alpha inhibition with PX-478 as studied by MR spectroscopy in vivo and ex vivo. NMR Biomed 2005;18(7):430-439.
11. Perou CM, Sorlie T, Eisen MB, van de Rijn M, Jeffrey SS, Rees CA, Pollack JR, Ross DT, Johnsen H, Akslen LA, Fluge O, Pergamenschikov A, Williams C, Zhu SX, Lonning PE, Borresen-Dale AL, Brown PO, Botstein D. Molecular portraits of human breast tumours. Nature 2000;406(6797):747-752.
12. Sorlie T, Perou CM, Tibshirani R, Aas T, Geisler S, Johnsen H, Hastie T, Eisen MB, van de Rijn M, Jeffrey SS, Thorsen T, Quist H, Matese JC, Brown PO, Botstein D, Lonning PE, Borresen-Dale AL. Gene expression patterns of breast carcinomas distinguish tumor subclasses with clinical implications. Proc Natl Acad Sci U S A 2001;98(19):10869-10874.
13. Podo F, Buydens LM, Degani H, Hilhorst R, Klipp E, Gribbestad IS, Van Huffel S, van Laarhoven HW, Luts J, Monleon D, Postma GJ, Schneiderhan-Marra N, Santoro F, Wouters H, Russnes HG, Sorlie T, Tagliabue E, Borresen-Dale AL. Triple-negative breast cancer: present challenges and new perspectives. Mol Oncol 2010;4(3):209-229.
14. Cespedes MV, Casanova I, Parreno M, Mangues R. Mouse models in oncogenesis and cancer therapy. Clin Transl Oncol 2006;8(5):318-329.
15. Vanhaesebroeck B, Guillermet-Guibert J, Graupera M, Bilanges B. The emerging mechanisms of isoform-specific PI3K signalling. Nat Rev Mol Cell Biol 2010;11(5):329-341.
16. Moulder SL. Does the PI3K pathway play a role in basal breast cancer? Clin Breast Cancer 2010;10 Suppl 3:S66-71.
17. Britten CD. PI3K and MEK inhibitor combinations: examining the evidence in selected tumor types. Cancer Chemother Pharmacol 2013.
18. Beloueche-Babari M, Jackson LE, Al-Saffar NM, Eccles SA, Raynaud FI, Workman P, Leach MO, Ronen SM. Identification of magnetic resonance detectable metabolic changes associated with inhibition of phosphoinositide 3-kinase signaling in human breast cancer cells. Mol Cancer Ther 2006;5(1):187-196.

19. Ward CS, Venkatesh HS, Chaumeil MM, Brandes AH, Vancriekinge M, Dafni H, Sukumar S, Nelson SJ, Vigneron DB, Kurhanewicz J, James CD, Haas-Kogan DA, Ronen SM. Noninvasive detection of target modulation following phosphatidylinositol 3-kinase inhibition using hyperpolarized 13C magnetic resonance spectroscopy. Cancer Res 2010;70(4):1296-1305.
20. Al-Saffar NM, Jackson LE, Raynaud FI, Clarke PA, Ramirez de Molina A, Lacal JC, Workman P, Leach MO. The phosphoinositide 3-kinase inhibitor PI-103 downregulates choline kinase alpha leading to phosphocholine and total choline decrease detected by magnetic resonance spectroscopy. Cancer Res 2010;70(13):5507-5517.
21. Bergamaschi A, Hjortland GO, Triulzi T, Sorlie T, Johnsen H, Ree AH, Russnes HG, Tronnes S, Maelandsmo GM, Fodstad O, Borresen-Dale AL, Engebraaten O. Molecular profiling and characterization of luminal-like and basal-like in vivo breast cancer xenograft models. Mol Oncol 2009;3(5-6):469-482.
22. Maira SM, Stauffer F, Brueggen J, Furet P, Schnell C, Fritsch C, Brachmann S, Chene P, De Pover A, Schoemaker K, Fabbro D, Gabriel D, Simonen M, Murphy L, Finan P, Sellers W, Garcia-Echeverria C. Identification and characterization of NVP-BEZ235, a new orally available dual phosphatidylinositol 3-kinase/mammalian target of rapamycin inhibitor with potent in vivo antitumor activity. Mol Cancer Ther 2008;7(7):1851-1863.
23. Moestue SA, Dam CG, Gorad SS, Kristian A, Bofin A, Maelandsmo GM, Engebraten O, Gribbestad IS, Bjorkoy G. Metabolic biomarkers for response to PI3K inhibition in basal-like breast cancer. Breast Cancer Res 2013;15(1):R16.
24. Payne GS, Troy H, Vaidya SJ, Griffiths JR, Leach MO, Chung YL. Evaluation of 31P high-resolution magic angle spinning of intact tissue samples. NMR Biomed 2006;19(5):593-598.
25. Marshall I, Higinbotham J, Bruce S, Freise A. Use of Voigt lineshape for quantification of in vivo 1H spectra. Magn Reson Med 1997;37(5):651-657.
26. Wider G, Dreier L. Measuring protein concentrations by NMR spectroscopy. J Am Chem Soc 2006;128(8):2571-2576.
27. Stewart JD, Marchan R, Lesjak MS, Lambert J, Hergenroeder R, Ellis JK, Lau CH, Keun HC, Schmitz G, Schiller J, Eibisch M, Hedberg C, Waldmann H, Lausch E, Tanner B, Sehouli J, Sagemueller J, Staude H, Steiner E, Hengstler JG. Choline-releasing glycerophosphodiesterase EDI3 drives tumor cell migration and metastasis. Proc Natl Acad Sci U S A 2012;109(21):8155-8160.
28. Ben-Yoseph O, Badar-Goffer RS, Morris PG, Bachelard HS. Glycerol 3-phosphate and lactate as indicators of the cerebral cytoplasmic redox state in severe and mild hypoxia respectively: a 13C- and 31P-n.m.r. study. Biochem J 1993;291 (Pt 3):915-919.
29. Moestue SA, Borgan E, Huuse EM, Lindholm EM, Sitter B, Borresen-Dale AL, Engebraaten O, Maelandsmo GM, Gribbestad IS. Distinct choline metabolic profiles are associated with differences in gene expression for basal-like and luminal-like breast cancer xenograft models. BMC Cancer 2010;10:433.
30. Dreier L, Wider G. Concentration measurements by PULCON using X-filtered or 2D NMR spectra. Magn Reson Chem 2006;44 Spec No:S206-212.
31. Barantin L, Le Pape A, Akoka S. A new method for absolute quantitation of MRS metabolites. Magn Reson Med 1997;38(2):179-182.
32. Albers MJ, Butler TN, Rahwa I, Bao N, Keshari KR, Swanson MG, Kurhanewicz J. Evaluation of the ERETIC method as an improved quantitative reference for 1H HR-MAS spectroscopy of prostate tissue. Magn Reson Med 2009;61(3):525-532.
33. Middleton DA, Bradley DP, Connor SC, Mullins PG, Reid DG. The effect of sample freezing on proton magic-angle spinning NMR spectra of biological tissue. Magn Reson Med 1998;40(1):166-169.
34. Sitter B, Lundgren S, Bathen TF, Halgunset J, Fjosne HE, Gribbestad IS. Comparison of HR MAS MR spectroscopic profiles of breast cancer tissue with clinical parameters. NMR Biomed 2006;19(1):30-40.
35. Bartholomeusz C, Gonzalez-Angulo AM. Targeting the PI3K signaling pathway in cancer therapy. Expert Opin Ther Targets 2012;16(1):121-130.

36. De Silva SS, Payne GS, Thomas V, Carter PG, Ind TE, deSouza NM. Investigation of metabolite changes in the transition from pre-invasive to invasive cervical cancer measured using (1)H and (31)P magic angle spinning MRS of intact tissue. NMR Biomed 2009;22(2):191-198.
37. Delikatny EJ, Lander CM, Jeitner TM, Hancock R, Mountford CE. Modulation of MR-visible mobile lipid levels by cell culture conditions and correlations with chemotactic response. Int J Cancer 1996;65(2):238-245.
38. Milkevitch M, Shim H, Pilatus U, Pickup S, Wehrle JP, Samid D, Poptani H, Glickson JD, Delikatny EJ. Increases in NMR-visible lipid and glycerophosphocholine during phenylbutyrate-induced apoptosis in human prostate cancer cells. Biochim Biophys Acta 2005;1734(1):1-12.
39. Hakumaki JM, Poptani H, Sandmair AM, Yla-Herttuala S, Kauppinen RA. 1H MRS detects polyunsaturated fatty acid accumulation during gene therapy of glioma: implications for the in vivo detection of apoptosis. Nat Med 1999;5(11):1323-1327.
40. Brandes AH, Ward CS, Ronen SM. 17-allyamino-17-demethoxygeldanamycin treatment results in a magnetic resonance spectroscopy-detectable elevation in choline-containing metabolites associated with increased expression of choline transporter SLC44A1 and phospholipase A2. Breast Cancer Res 2010;12(5):R84.
41. Delikatny EJ, Chawla S, Leung DJ, Poptani H. MR-visible lipids and the tumor microenvironment. NMR Biomed 2011;24(6):592-611.
42. Brachmann SM, Hofmann I, Schnell C, Fritsch C, Wee S, Lane H, Wang S, Garcia-Echeverria C, Maira SM. Specific apoptosis induction by the dual PI3K/mTor inhibitor NVP-BEZ235 in HER2 amplified and PIK3CA mutant breast cancer cells. Proc Natl Acad Sci U S A 2009;106(52):22299-22304.
43. Valonen PK, Griffin JL, Lehtimaki KK, Liimatainen T, Nicholson JK, Grohn OH, Kauppinen RA. High-resolution magic-angle-spinning 1H NMR spectroscopy reveals different responses in choline-containing metabolites upon gene therapy-induced programmed cell death in rat brain glioma. NMR Biomed 2005;18(4):252-259.
44. Iorio E, Ricci A, Bagnoli M, Pisanu ME, Castellano G, Di Vito M, Venturini E, Glunde K, Bhujwalla ZM, Mezzanzanica D, Canevari S, Podo F. Activation of phosphatidylcholine cycle enzymes in human epithelial ovarian cancer cells. Cancer Res 2010;70(5):2126-2135.
45. Begley JK, Redpath TW, Bolan PJ, Gilbert FJ. In vivo proton magnetic resonance spectroscopy of breast cancer: a review of the literature. Breast Cancer Res 2012;14(2):207.
46. Bathen TF, Heldahl MG, Sitter B, Vettukattil R, Bofin A, Lundgren S, Gribbestad IS. In vivo MRS of locally advanced breast cancer: characteristics related to negative or positive choline detection and early monitoring of treatment response. MAGMA 2011;24(6):347-357.

Figures legend and Tables

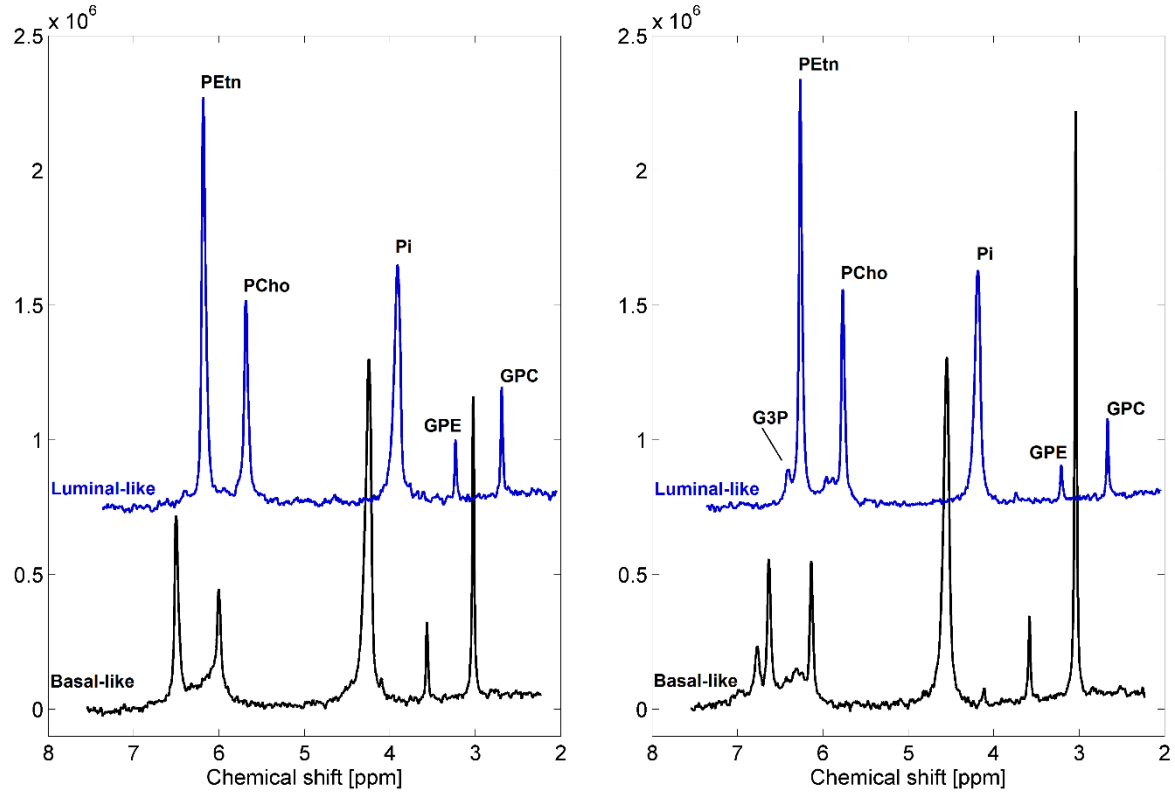

Figure 1: The ^{31}P metabolite profiles from basal- and luminal xenografts before and after BEZ235 treatment: Representative ^{31}P HR-MAS spectra of BEZ235-treated tissues (right) and controls (left). In basal-like xenografts (black), BEZ235 treatment induced a significant decrease in PEtn concentration whilst PCho and GPC signals are significantly increased compared with controls. Basal-like xenografts could be discriminated from luminal-like xenografts (blue) by a lower PCho-GPC ratio and lower PEtn concentration. In spectra obtained from BEZ235-treated samples glycerol-3-phosphate (G3P) was detected at about 6.8 ppm (The luminal-like spectra are shifted slightly to the right for visualization purpose). The chemical shift was calibrated to the GPC peak at 3.04 ppm.

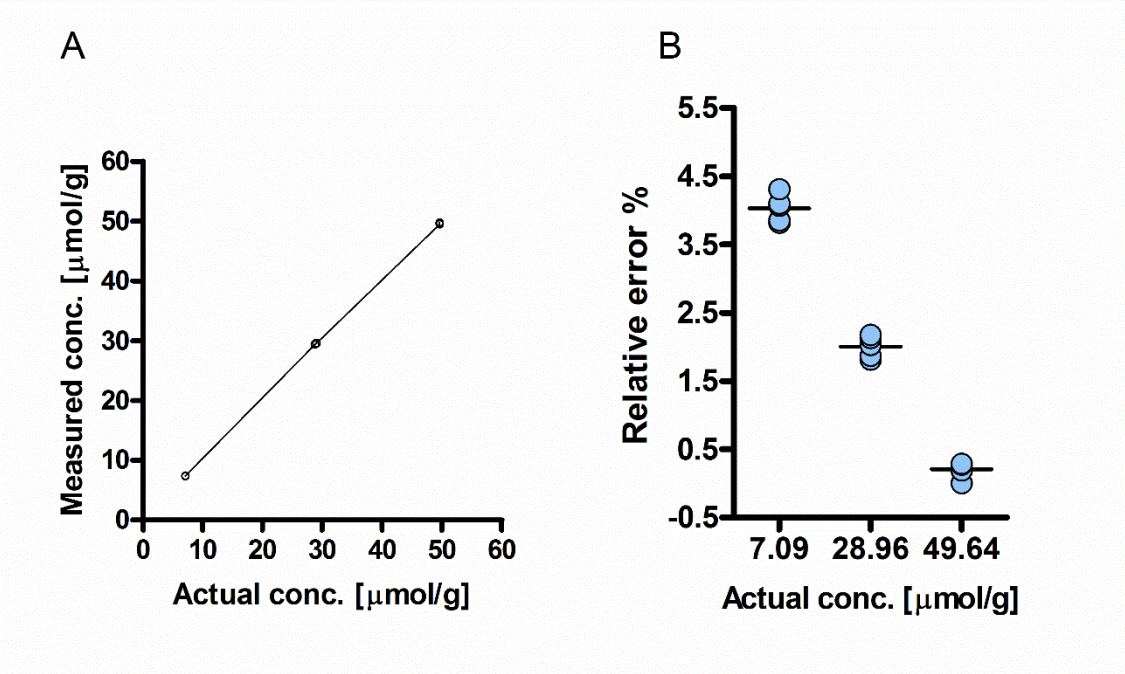

Figure 2: Accuracy and precision of the MDPA calibration standard curve. Actual MDPA concentrations versus the measured MDPAs are plotted, using the highest MDPA concentration as reference (A). A linear regression was performed on the data demonstrating a significant correlation ($P < 0.0001$ and r = 0.96) between actual and measured concentrations. The relative error plot (B) is a measure of the method's accuracy, and indicates the agreement between the actual and the measured concentrations of MDPAs (B).

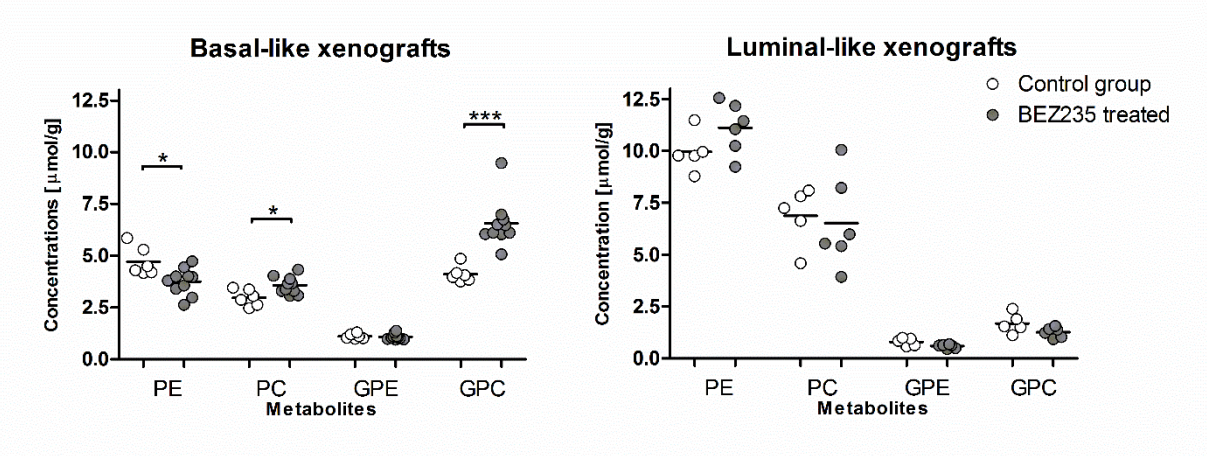

Figure 3: Effect of BEZ235 treatment on the phosphorylated metabolite concentrations (µmol/g) in basal- and luminal-like xenograft tumors. *: $P < 0.05$, ***: $P < 0.001$.

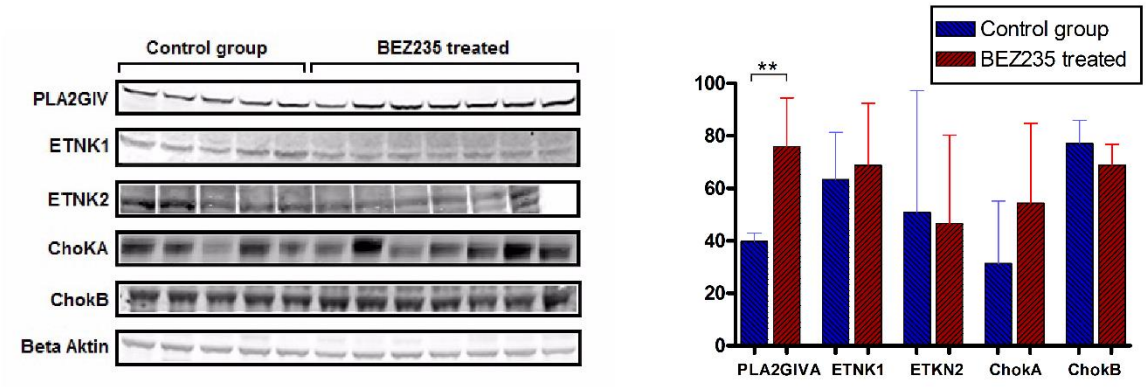

Figure 4: Phospholipase A2 group IV expression was increased after BEZ235 treatment in basal-like xenografts. The bar graph shows the quantification of the immunoblots (mean ± SD). Phospholipase A2 group IV (PLA2GIV), Ethanolamine kinase 1 and 2 (ETNK1/2), Choline kinase alpha/beta (ChoKA/B), and β-actin protein expression were examined by immunoblotting of tissue samples after MRS experiments (control group (n = 5) and BEZ235-treated group (n = 7)). This demonstrated a higher expression of PLA2GIV protein (*P* = 0.005), but no changes in ETNK1 and ChoKA/B in samples from basal-like xenografts treated with BEZ235.

Table 1: ^{31}P chemical shifts and longitudinal relaxation times (T1). The ^{31}P resonances determined in MR spectra of intact tissues from luminal- and basal-like breast cancer xenografts.

			n	G3P	PEtn	PCho	Pi	GPE	GPC
Chemical shift [ppm]	Luminal-like	Control	5	Nd	6.49±0.07	5.99±0.07	4.19±0.10	3.58±0.00	3.04±0.00
		BEZ235	6	6.78±0.061	6.62±0.04	6.13±0.04	4.51±0.12	3.58±0.00	3.04±0.00
	Basal-like	Control	6	Nd	6.57±0.04	6.07±0.04	4.35±0.09	3.58±0.00	3.04±0.00
		BEZ235	10	6.75±0.04	6.63±0.02	6.13±0.02	4.52±0.05	3.58±0.00	3.04±0.00
T1 [s]				Nd	1.52±0.50	1.56±0.53	1.12±0.28	1.25±0.36	1.07 ±0.06

Nd; not determined.

Table 2: Stability of the phosphorylated metabolites: Metabolite peak areas were measured using ^{1}H HR-MAS MRS before and after the ^{31}P HR-MAS MRS analysis. The table shows the increase (% of pre-analysis value, mean ± SD) in PCho and GPC during ^{31}P HR-MAS analysis. **: Significant difference between basal-like and luminal-like xenografts, P = 0.007.

Xenografts		n	GPC	PCho
Basal-like	BEZ235	5	15.66 ± 3.55	18.80 ± 5.33**
	Control	6	13.16 ± 1.99	16.61 ± 5.42
Luminal-like	BEZ235	6	11.08 ± 4.82	10.20 ± 4.52**
	Control	10	09.70 ± 3.21	10.52 ± 2.33